



CHAPTER IV

SILVER INCLUSION POLYBENZOXAZINE XEROGEL MEMBRANE FOR CO₂/CH₄ SEPARATION

4.1 Abstract

The effect of silver ion incorporated with a novel organic polybenzoxazine xerogel (PBZ) was investigated as a membrane for flue gas separation. The fully cured interconnected polybenzoxazine xerogel was impregnated with silver nitrate solution. The exothermic peak of polybenzoxazine disappeared after being fully polymerized as observed by DSC. FT-IR results indicated the chemical reaction between the N-Ag. The char yield of Ag⁺-included in the polybenzoxazine membrane increased rapidly with the increasing of the metal salt concentrations which might be due to the complex formation between metal ions and polybenzoxazine, resulting in more stable cyclic compounds that could form char during the heat treatment. However, the BET results and SEM micrographs showed no change in physical properties of PBZ after Ag⁺ inclusion. (The ideal separation of flue gas (CO₂, N₂ and CH₄) has been investigated). Interestingly, the CO₂/CH₄ selectivity was also increased with the incorporation of Ag⁺ ion since CO₂ molecules containing double bonds could react reversibly with these noble metal ions to form the π -bonded complex, thus obtaining good separation performance.

Keywords: Carbon membrane/ Polybenzoxazine/ Flue gas separation/ Silver inclusion

4.2 Introduction

Flue gases, normally produced by coalbed gas, consist of mixtures of methane (CH_4), carbon dioxide (CO_2), nitrogen (N_2), and heavier hydrocarbons ($>\text{C}_2$). CO_2 is considered to be crucial greenhouse gas that has a direct impact on the global atmosphere [1]. The emission of CO_2 has resulted in not only the increasing of the world temperature and weather disaster but also considered as hazardous matter to human health [2].

To produce high-purity energy products, gas separation technique by membrane is the attractive approach because of its low capital investment, simplicity and ease of installation and operation, low maintenance requirements, low weight and space requirement, and good process flexibility [3].

One of the most important elements in gas separation technique is the mix matrix membranes (MMMs), consisting of organic polymer and inorganic particle phase which has the molecular sieve characteristics [4]. However, when using MMMs; the interfacial interaction between two phases: molecular sieve and polymeric phase has to be concerned [5]. Additionally, the CO_2 -induced plasticization effect can decrease the membrane selectivity [6].

Therefore, inorganic membranes; e.g. zeolite, alumina, carbon, have been investigated to solve the problems associating with MMMs which will also improve the gas separation performance [7]. Moreover, inorganic membranes have excellent thermal and chemical stability, well-defined stable pore structure than polymeric membranes and no CO_2 -induced plasticization effect [8-10].

Among inorganic membranes, we consider carbon membrane to be most attractive since it can be prepared by pyrolysis of various polymer precursors such as polyimides [11], polyacrylonitrile [12], poly(furfuryl alcohol) [13], phenolic resin [14,15] and etc. As a result, the membrane fabrication is much more economical than other inorganic membranes due to easy processibility.

In this study, polybenzoxazine, which is a high-performance thermosetting resin, was selected as a precursor to prepare carbon membrane since it exhibits

excellent properties such as low shrinkage after curing, low water absorption, good thermal stability and high glass transition temperature [16].

The purpose of this work was to develop a new carbon membrane by using polybenzoxazine thermosetting resin as a polymeric precursor with silver inclusion for flue gas separation. The incorporation of Ag⁺ ions enable the formation of reversible π -bonded complex with the double bonds CO₂ and hydrocarbon gases, resulting in enhanced separation performance.

4.3 Experimental

4.3.1 Materials

All chemicals were used without further purification. Bisphenol-A was purchased from Aldrich, Germany. Triethylenetetramine (TETA) was purchased from FACAI Group Limited, Thailand. Formaldehyde solution (37% by weight) was purchased from Merck, Germany. *N,N*-Dimethylformamide (DMF) was purchased from Labscan Asia Co., Ltd., Thailand and Silver Nitrate (AgNO₃) was purchased from Fisher Scitific, UK.

4.3.2 Measurements

The curing behavior of the benzoxazine and the decomposition temperature range of the polybenzoxazine precursor were investigated by using a PerkinElmer Differential Scanning Calorimeter, DSC 7, analyzer to get useful synthesis parameters for the polybenzoxazine precursor. Approximately 5–9 mg samples were sealed in aluminum pans. The sample was heated from ambient temperature to 300 °C at a heating rate of 10 °C/min under nitrogen flow rate of 10 ml/min. Thermogravimetric analysis was also conducted with Perkin Elmer Thermogravimetric/Differential Thermal Analyzer (TG-DTA) where the sample was heated from ambient temperature to 900 °C at a heating rate of 20 °C/min under nitrogen flow rate of 50 ml/min. FT-IR spectra of polybenzoxazine precursor and silver inclusion polybenzoxazine were recorded on a Nicolet Nexus 670 FT-IR

spectrometer using KBr pallet technique. The field emission scanning electron microscope (FE-SEM, HITACHI S4800) was used to study the microstructure of polybenzoxazine xerogel and carbon xerogel, the samples were coated with platinum under vacuum prior to investigation. Furthermore, the amount of Ag^+ on the surface can be determined by EDX mode. Elemental analysis of the silver inclusion polybenzoxazine, particularly investigate by Axios WD XRAF, Panalytical. BET surface area and pore size distribution of both organic and carbon xerogels were calculated from nitrogen adsorption isotherms at 77 K using a Quantachrome/Autosorb-1 Surface Area Analyzer based on the Brunauer–Emmett–Teller (BET) and Barret-Joyner-Halenda (BJH) methods, respectively.

In this study, CO_2 , N_2 (Prax Air) and CH_4 (TIG) were used as testing gases for all membranes. All tested gases were of a high purity (HP) grade and used as received. A schematic diagram of the system used to carry out the gas permeability experiments is shown in Figure 4.1.

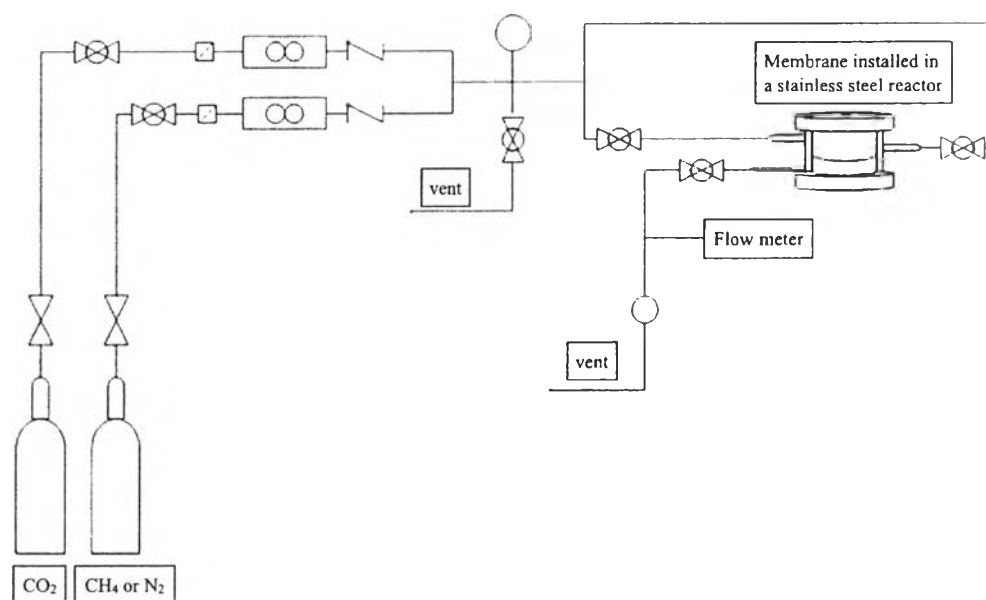


Figure 4.1 Experimental set up for the gas permeability apparatus.

The experiments were conducted at room temperature under an absolute pressure of 34.59 psia. (Absolute pressure = gauge pressure 20 psig + local atmospheric pressure 14.59 psi) The area of the membrane in contact with the gas was 0.5024 cm². The testing gas was flowed for 1 hour in order to get equilibrium state. The

equilibrium state was obtained by measuring the constant permeate rate. Once reached the steady-state, individual gas flow rate was measured using an ADM1000 universal gas flow meter, Agilent technology. The results of each sample were determined from an average of at least 3 tests. The attained data were used to calculate the gas selectivity and permeability. The ideal separation factor (Gas Selectivity, $S_{A/B}$) for component A and B is defined as the ratio of permeance of each component as shown in equation 1:

$$S_{A/B} = \frac{P_A}{P_B} \quad (1)$$

The permeance for the permeated gas can be obtained by equation 2:

$$\left(\frac{P}{\delta}\right)_i = \frac{Q_i \times 14.7 \times 10^6}{(A) \times (\Delta P) \times 76} \quad (2)$$

Where; $\left(\frac{P}{\delta}\right)_i$ = permeance of gas 'i' (GPU),

P = permeability of gas 'i' ($10^{-10} \text{ cm}^3 \text{ (STP) cm/cm}^2 \text{ s cm Hg}$)

(1 Barrer = $10^{-10} \text{ cm}^3 \text{ (STP) cm/cm}^2 \text{ s cm Hg} = 7.5 \times 10^{-18} \text{ m}^2 \text{ s}^{-1} \text{ Pa}^{-1}$),

δ = thickness of membrane (μm),

Q_i = volumetric flow rate of gas 'i' (cm^3/sec),

A = membrane area (cm^2), and

ΔP = pressure difference between the feed side and the permeating side (psia).

4.3.3 Methodology

4.3.3.1 Synthesis of the benzoxazine precursor

The benzoxazine precursor was synthesized by dissolving bisphenol-A (2.28 g) in DMF (12.97 ml), followed by adding formaldehyde (3.24 g) and TETA (1.46 g). The mixture was stirred continuously for 1 h while the reaction was cooled with an ice bath until a homogeneous yellow viscous liquid was obtained. The mole ratio of bisphenol-A: formaldehyde:diamine was 1:4:1.

4.3.3.2 Preparation of polybenzoxazine xerogel

The benzoxazine precursor was transferred into vials and sealed before being placed in an oil bath. The samples were heated in the oil bath at 80 °C for 48 h in a closed system, followed by evaporating the solvent at ambient conditions for one day.

4.3.3.3 Preparation of polybenzoxazine xerogel membranes

After the organic xerogel was evaporated over night, it was cut by the diamond blade low speed cutter machine with the thickness of 2 mm, and the rotor speed of 450 rpm. The obtained organic xerogel was then fully cured by step curing in an oven at 140°, 160°, and 180 °C for 2 h at each temperature and then at 200 °C for 3 h. The synthetic reaction is shown in Figure 4.2.

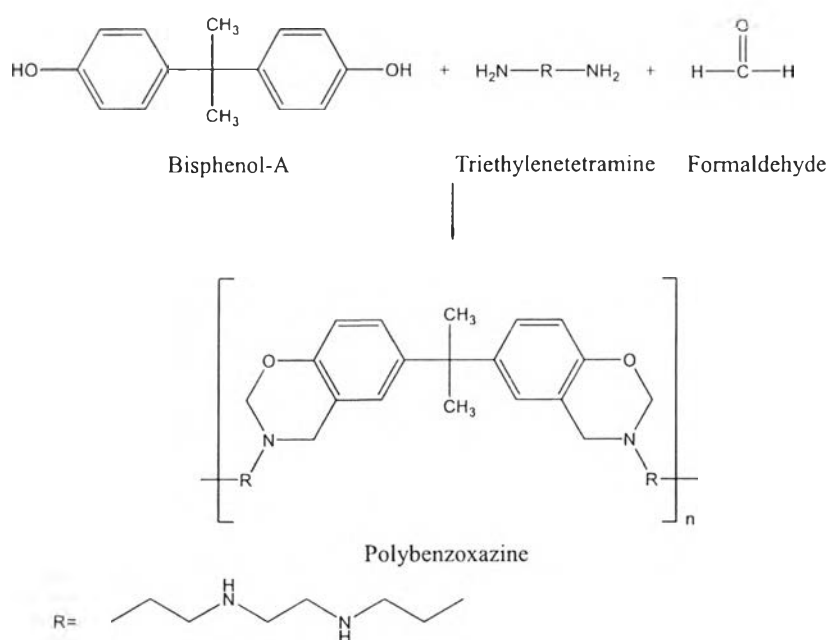


Figure 4.2 Preparation of polybenzoxazine precursor.

4.3.3.4 Preparation of silver-polybenzoxazine based xerogel

The fully cured PBXZs were impregnated in 0.5 and 1.0 mol/dm³ aqueous AgNO₃ solution (abbreviated as 0.5PBZX-Ag and 1.0PBZX-Ag, respectively). The solution was stirred for 1 day at 60–70°C in a temperature-controlled water bath. After the reaction, PBZX with silver ion was washed with of

500 mL deionized water to remove all the unreacted cations, before dried at 100°C overnight [17]. The structural characteristics of silver-polybenzoxazine based xerogel were identified by using FTIR. The silver inclusion polybenzoxazine structure shown in Figure 4.3.

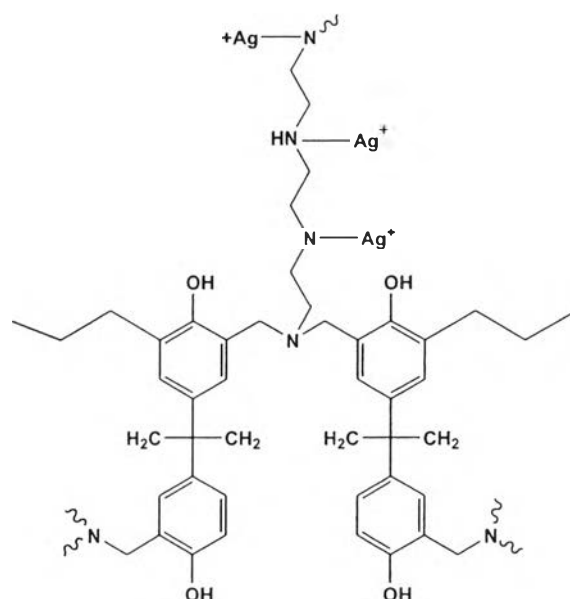


Figure 4.3 Silver inclusion polybenzoxazine structure.

4.3.3.5 Preparation of Polybenzoxazine and Silver-Polybenzoxazine based Xerogel Carbon

In order to prepare the carbon membranes, the PBZX, 0.5PBXZ-Ag and 1.0PBZX-Ag membranes were carbonized in a quartz reactor under nitrogen flow at 500 cm³/min, using the following ramp cycle: 30–250 °C in 60 min, 250–600 °C in 300 min, 600–800 °C in 60 min, and holding at 800 °C for 60 min. Then, the furnace was cooled down to room temperature under nitrogen atmosphere.

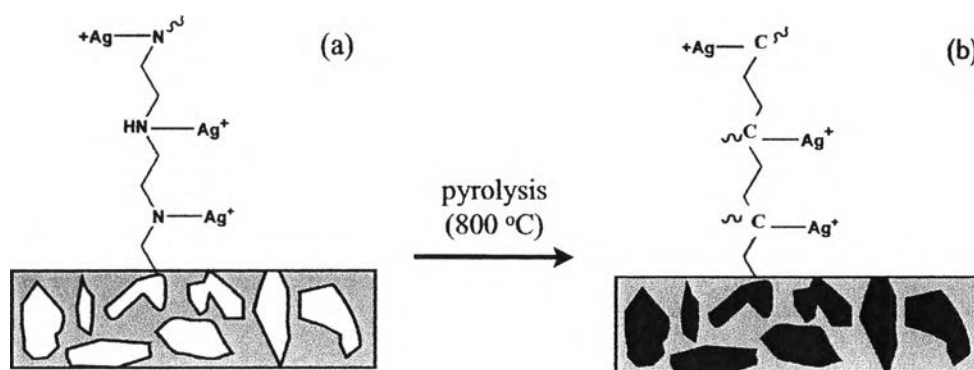


Figure 4.4 The formation of carbon-silver membrane.

4.3.3.6 Characterization of Polybenzoxazine Precursor, Silver inclusion polybenzoxazine and carbon xerogel

The chemical structure of benzoxazine precursor was characterized by Fourier transform infrared (FT-IR) spectroscopy. The thermal behaviors were measured using DSC and TG-DTA.

The surface area of carbon aerogels and activated carbon aerogels were calculated from nitrogen adsorption isotherms at 77 K based on the Brunauer–Emmett–Teller (BET) method and the pore size distribution was calculated with the adsorption data based on the Barret-Joyner-Halenda method (BJH). The surface morphology was characterized using scanning electron microscope (SEM).

4.4 Results and discussion

4.4.1 Thermal Behaviors of Polybenzoxazine Precursors

The thermal behavior of polybenzoxazine and benzoxazine precursor confirmed that the polymerization of benzoxazine occurred. Figure 4.5 (a) shows the exothermic peak from 200-270 °C of benzoxazine precursor while the exothermic peak of polybenzoxazine disappeared as shown in Figure 4.5 (b). These obviously show that the polymerization of benzoxazine precursor by ring-opening of oxazine was taken place. This result was similar to that reported by Takeichi and coworker [18].

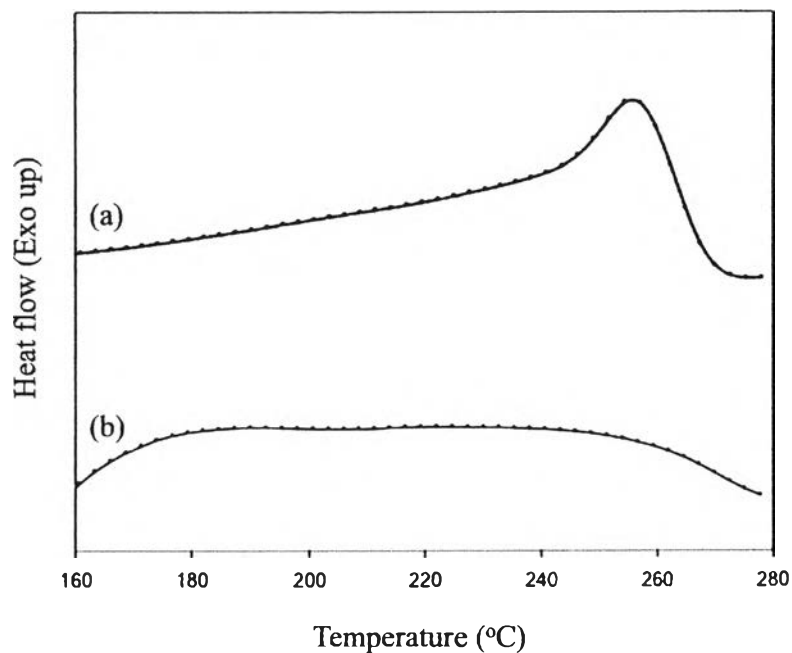


Figure 4.5 DSC thermograms of (a) the polybenzoxazine precursor after drying at 80°C (pre-cured) and (b) after heat treatment at 200 °C (fully-cured).

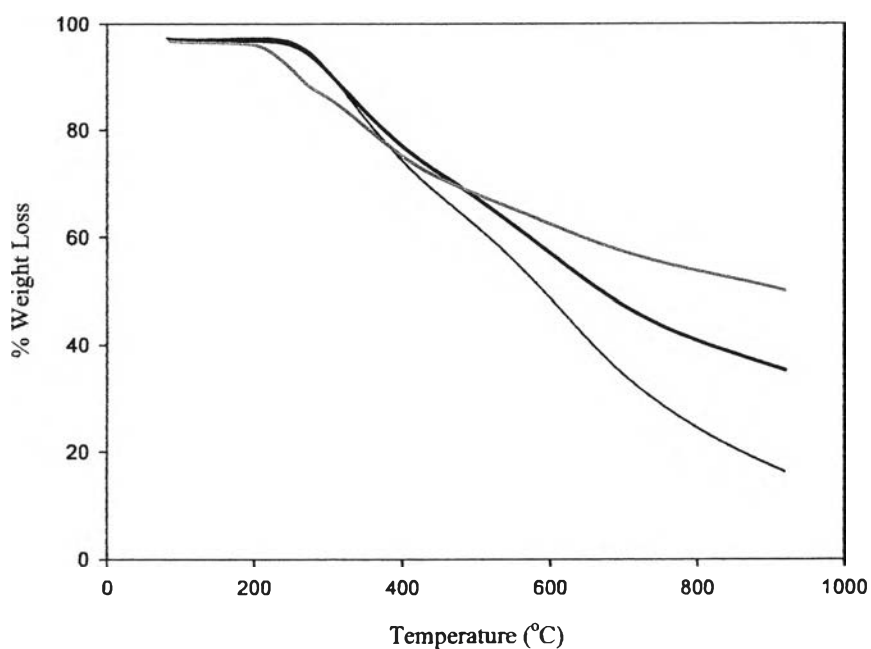


Figure 4.6 TGA thermogram of PBZ xerogels (—), PBZ xerogels impregnated with 0.5M AgNO₃ (---) and PBZ xerogels impregnated with 1.0 M AgNO₃ (· · ·).

From Figure 4.6, the decomposition temperature began at 260°C with the maximum mass loss rate in the temperature range of 260-600°C. The result was in accordance with our previous study [19]. The thermal decomposition temperature was enhanced for the PBZ xerogel impregnated with AgNO₃ and the effect was noticeable with increased with increasing the amount of Ag ions content. In addition, the char yield of the PBZ xerogel impregnated with AgNO₃ was significantly increased. These results indicate that the thermal stability of AgNO₃ impregnated with PBZX was influenced by the silver incorporation which is in agreement with the study of Ruban *et al.* In addition, the char yield increased rapidly with the concentration of metal salt aqueous solution. The possible explanation for this observation might be due to the silver ions entrapment by benzoxazines, leading to the co-ordination complex formation corresponding to the results reported in the previous work on the improvement of the thermal stability of polybenzoxazine by transition metals [20].

4.4.2 The Chemical Structure of Polybenzoxazine Precursors

The chemical structure of benzoxazine precursor was examined by FTIR spectra as shown in Figure 4.7a. The characteristic absorption bands at 1234-1238 cm⁻¹ (asymmetric stretching of C-O-C of oxazine), 1187 cm⁻¹ (asymmetric stretch of C-N-C) and 1334-1340 cm⁻¹ (CH₂ wagging) were observed (Figure 4.7(a)). Additionally, the characteristic absorption assigned to the stretching of trisubstituted benzene ring at 1511 cm⁻¹ and the out-of-plane bending vibrations of C-H at 943-949 cm⁻¹ were detected, indicating the presence of the cyclic benzoxazine structure in the backbone of the precursor [21]. After polymerization at 200 °C, the intensity of those characteristic absorption bands decreased due to the ring opening polymerization was completed as shown in Figure 4.7 b [18].

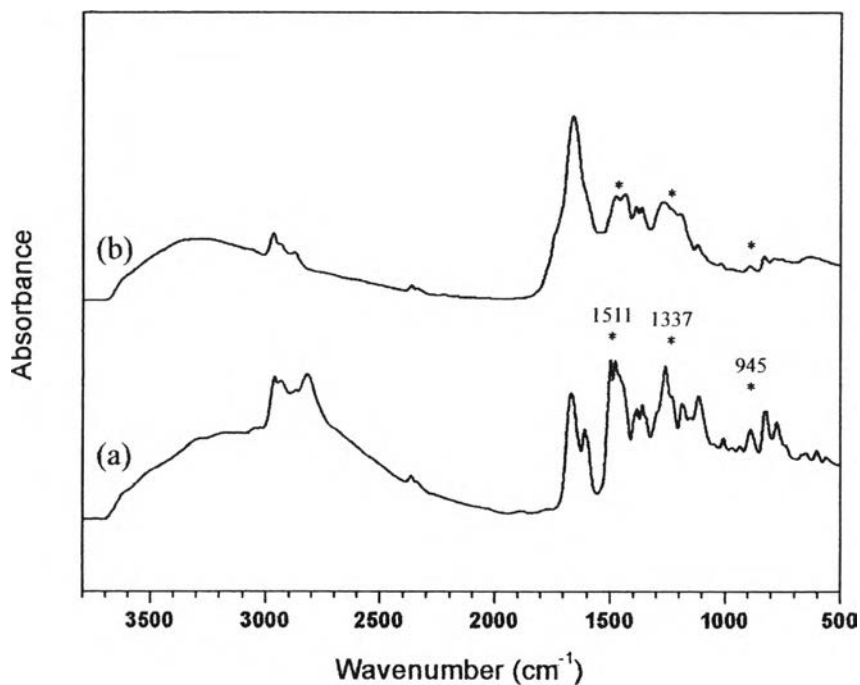


Figure 4.7 FTIR spectra of (a) polybenzoxazine precursors and (b) fully-cured polybenzoxazine.

In additions, the FTIR spectra of the PBZ xerogel impregnated with AgNO_3 are shown in Figure 4.8b and 4.8c. The Schiff base and secondary amide are known to form complex with metals. The band at 3370 cm^{-1} assigned to NH_2 stretching. The position of these bands changed during complex formation. The shifting of the band to 3350 cm^{-1} was observed. The absorption band at 1385 cm^{-1} shows a stronger intensity when Ag^+ ion was incorporated in the structure indicating, CH_2 wagging vibration of amine and silver complex. This result supported the study of Low *et al.*, 2005 [22].

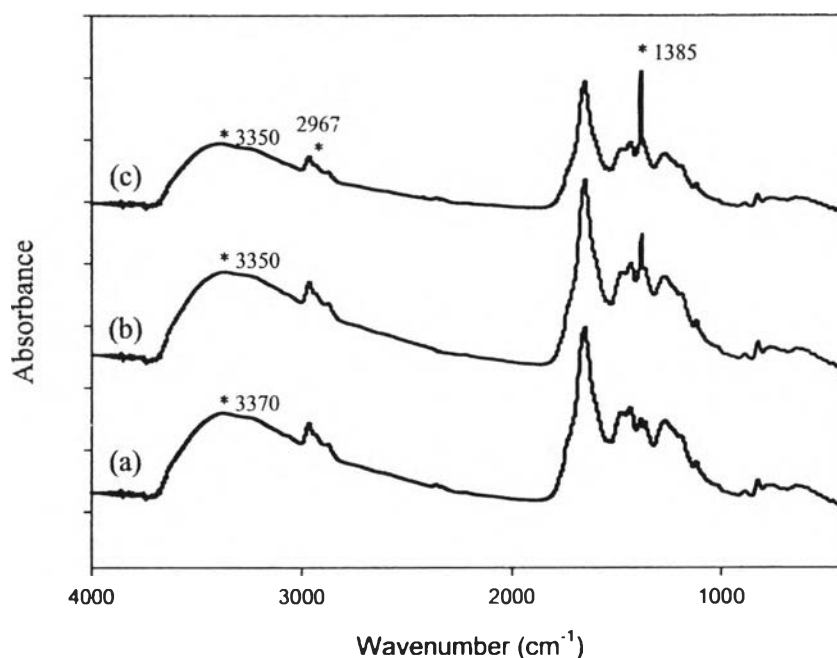


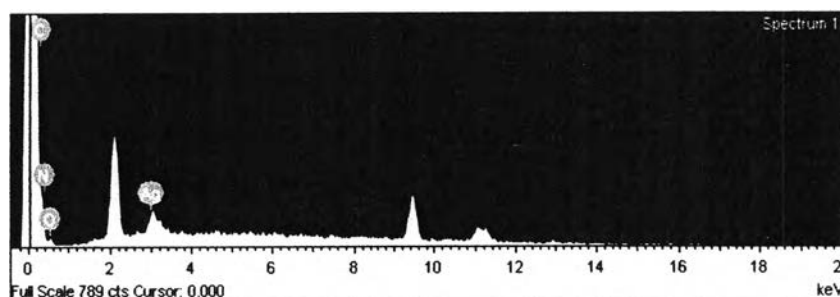
Figure 4.8 FTIR spectra of (a) polybenzoxazine, 0.5PBZX-Ag and (c) 1.0PBZ-Ag.

4.4.3 Polybenzoxazine Xerogel Impregnated with AgNO_3 Characterizations

To determine whether the silver ion incorporated with PBZ xerogel is actually successful, the measurement of the elemental composition of the PBZxerogel surface before and after the Ag-impregnated was performed by SEM-EDX instrument. EDX spectrum (Figure 4.9) demonstrates that silver ions have been incorporated after PBZ was impregnation in the aqueous AgNO_3 solution. Moreover, Table I shows that the higher the AgNO_3 concentration, the higher the Ag ion was found on the surface. The EDX results are supported that Ag ions were incorporated in the PBZ structure as shown in FTIR spectrum (Figure 4.9).

Table 4.1 EDX measurements of the surface of 0.5PBZX-Ag and 1.0PBZX-Ag

Elements	Atomic%	
	0.5PBZX-Ag	1.0PBZX-Ag
C	53.5	54.8
N	36.1	36.8
O	9.90	7.90
Ag	0.45	0.53

**Figure 4.9** EDX spectrum of 1.0PBZX-Ag

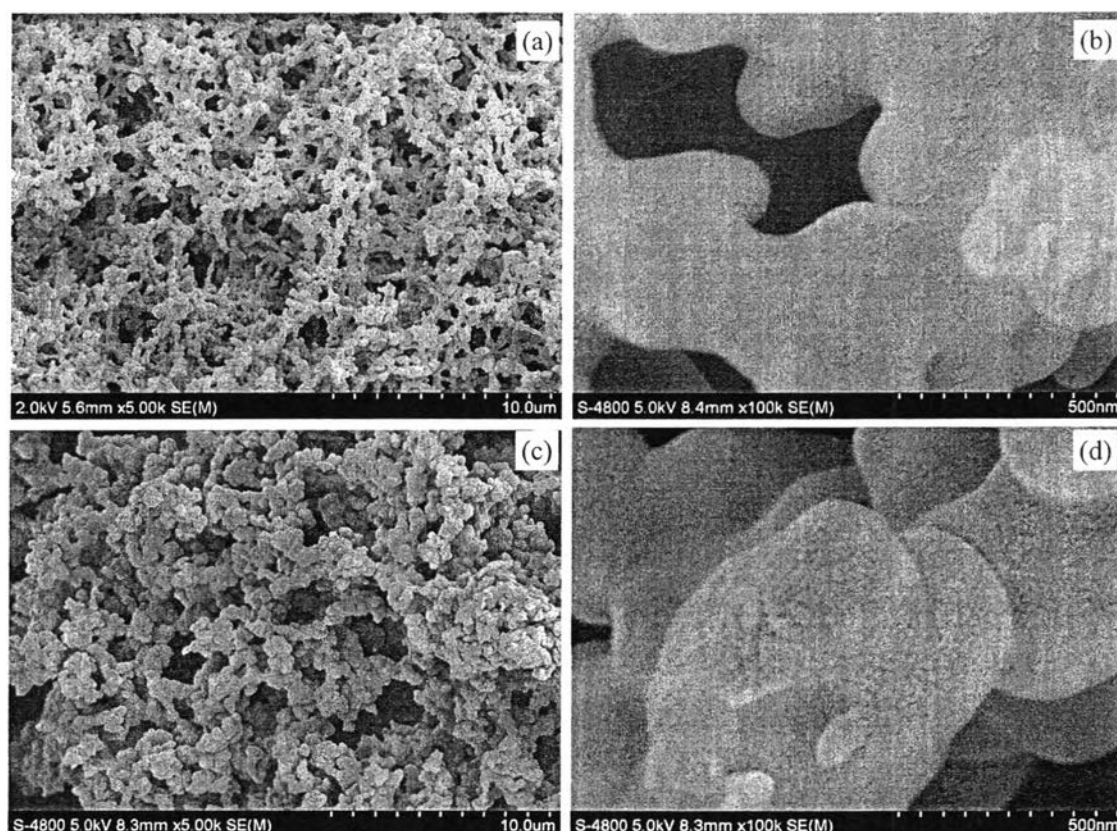
In addition, the measurement of the energy and intensity of the characteristic photons emitted from the sample was used to determine the amount of silver ion in the PBZ xerogel. The XRF principle enables the identification of the elements presenting in the sample and the determination of their mass or concentration. The XRF results indicated that only the Ag^+ was obtained implying that no oxidation reaction took place during the Ag-impregnated PBZX preparation processes. The amounts of silver concentration of 0.5PBZX-Ag and 1.0 PBZX-Ag compared to oxygen concentration are approximately 3.2% and 6.5%, respectively.

4.4.4 Morphology of Polybenzoxazine Xerogels and Carbon Xerogels

Figure 4.10 shows SEM micrographs of the organic xerogel and carbon xerogel which exhibit the 3D interconnected particles into a network with continuous open macropores. This result agrees with the study of Parkpoom *et al.*, [23] which studied the porous structure of polybenzoxazine-based organic aerogel.

However, in case of carbon xerogel, the denser porous structure was obtained. Since during pyrolysis process, some organic moieties in organic xerogel structure were decomposed resulting in sparser in carbon xerogel. In additions, when carbon xerogel and organic xerogel were compared with a magnification of 100k (Figure 4.10b and 4.10f), the carbon xerogel exhibits the sphere particles that combined together which provided the mesoporous structures.

In case of the impregnated AgNO_3 with PBZ xerogel (Figure 4.10c, 4.10d) and pyrolysis to become a carbon-silver xerogel (Figure 4.10g, 4.10h), the micrograph also shows similar morphology compared with the neat PBZ xerogel and carbon xerogel.



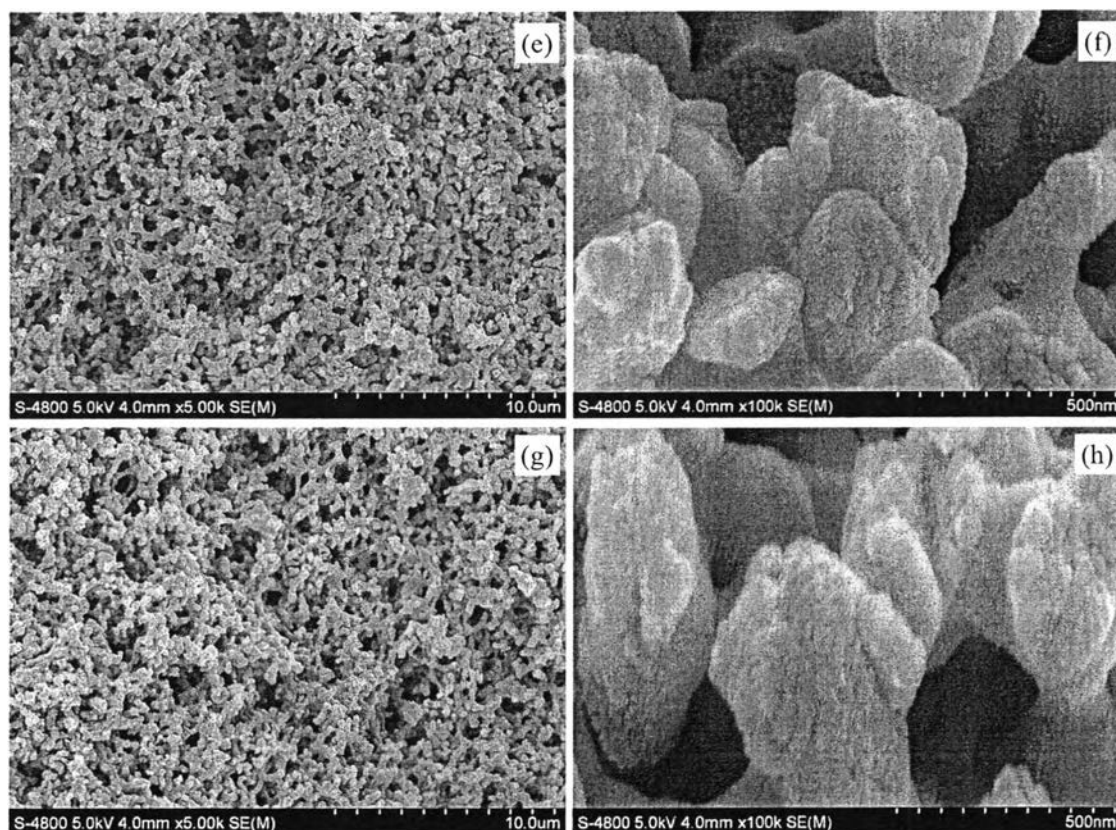


Figure 4.10 SEM micrographs of synthesized PBZ xerogel with a magnification of 5.0 k (a) and 100.0 k (b), PBZ xerogel impregnated with 1.0M AgNO_3 with a magnification 5.0 k (c) and 100.0 k (d), carbon xerogel with a magnification of 5.0 k (e) and 100.0 k (f) and carbon based silver impregnated with a magnification of 5.0 k (g) and 100.0 k (h).

4.4.5 Microstructure of PBZ-based Carbon Xerogels

The surface area, pore volume and pore diameter of organic xerogels and carbon xerogels are summarized in Table 4.2. It can be seen that the carbon xerogel had high surface area with large amount of mesopores and micropores, whereas the organic xerogels showed lower surface area, but larger pore size. After the organic xerogels were pyrolysed under nitrogen at 800 °C, the micropores and mesopores were introduced into the carbon xerogel, resulting in high surface area. For the organic xerogels with impregnated with 1.0M of AgNO_3 aqueous solution and after Ag^+ impregnated carbon xerogels, the surface area and porosity were similar to those of neat polybenzoxazine and pristine carbon xerogels. Furthermore, all the organic and carbon xerogels had an average pore diameter larger than an average

mesopore diameter, indicating that macropores are present as confirmed by the N_2 adsorption isotherm in Fig. 4.11-4.12, in which the adsorption branch did not reach the plateau region at the high relative pressure [24]. However, large macropores could not be detected by N_2 adsorption due to the limitation of the Kelvin equation [25-27].

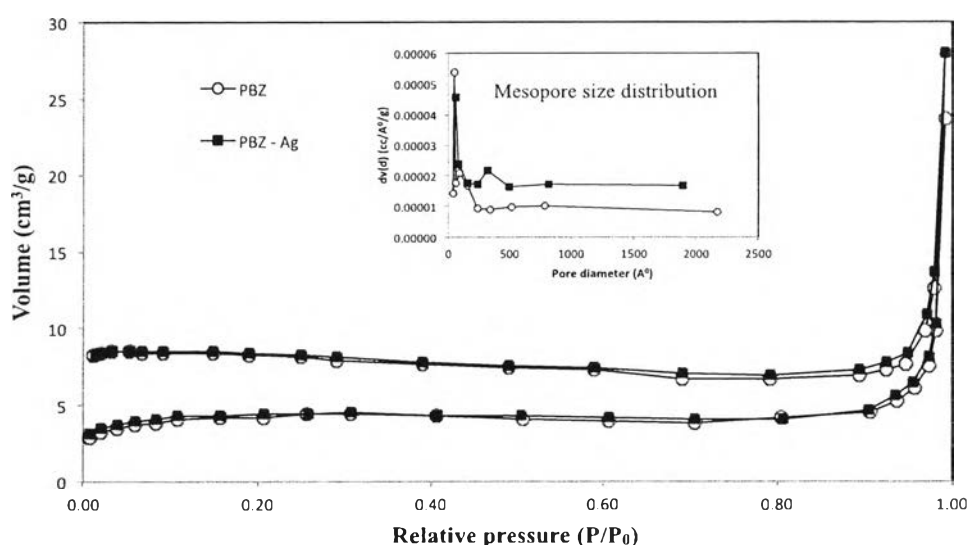


Figure 4.11 Adsorption isotherms of PBZ xerogels (○) and PBZ xerogels impregnated with 1.0M of $AgNO_3$ (■) prepared from benzoxazine precursor.

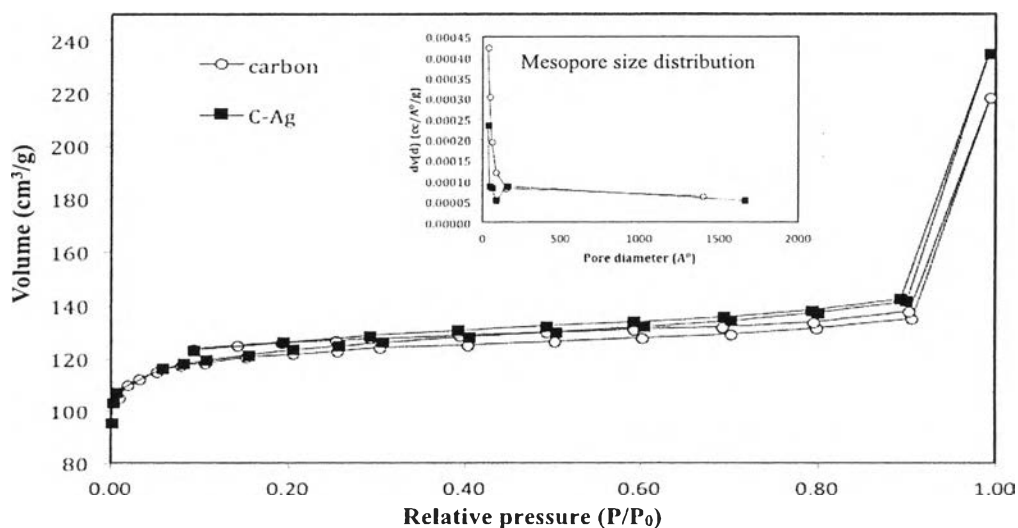


Figure 4.12 Adsorption isotherms of PBZ-based carbon xerogels (○) and pyrolyzed PBZ xerogels impregnated with 1.0M $AgNO_3$ (■) prepared from benzoxazine precursor [24].

Table 4.2 Pore structure of PBZX and PBZ-based carbon xerogels

Parameter	PBZX	1.0PBZX-Ag	CX	1.0CX-Ag
BET surface area (m ² /g)	13	14	370	375
Mesopore surface area (cm ² /g)	0.051	0.046	13	16
Micropore volume (cm ³ /g)	-	-	0.17	0.15
Mesopore volume (cm ³ /g)	0.03	0.03	0.16	0.17
Total pore volume (cm ³ /g)	0.04	0.04	0.34	0.35
Average micropore diameter (nm)	1.72	1.72	1.28	1.22
Average mesopore diameter (nm)	10	10	3.58	3.57
Average pore diameter (nm)	11	13	3.64	4.04

4.4.6 Gas Permeability

Carbon membranes based polybenzoxazine xerogel were tested in the single gas measurements. The permeability of these membranes was obtained in the sequence of CH₄, N₂ CO₂ at room temperature and 20 psi. The permeability and selectivity of CO₂, CH₄ and N₂ in carbon membranes and carbon-silver membrane are depicted in Figure 4.13–4.14.

4.4.6.1 *The effect of silver inclusion on the CO₂, CH₄ and N₂ permeability*

Carbon-silver based polybenzoxazine membranes were successfully fabricated with differences AgNO₃ concentration. Their CO₂, CH₄ and N₂ permeability is shown in Figure 4.6

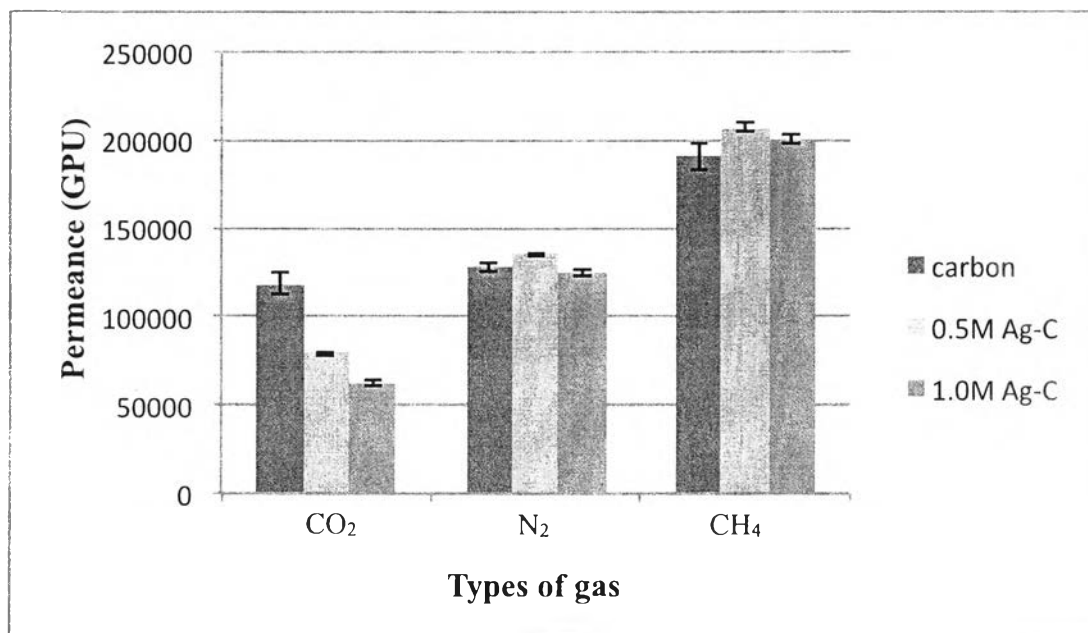


Figure 4.13 Effects of Silver Nitrate concentration on CO₂, CH₄ and N₂ permeability.

Figure 4.13 shows that the CO₂, CH₄ and N₂ permeabilities of carbon membrane and carbon-silver membrane depending on molecular kinetic diameters. The molecular kinetic diameters of CO₂, N₂ and CH₄ are 3.3 Å, 3.6 Å and 3.8 Å, respectively. Due to the configurational diffusion, the small difference in molecular size between CO₂, CH₄ and N₂ results in a big difference in the rate of diffusion through the interconnected porous membrane; the diffusion of CH₄ is faster than that of N₂ and CO₂. Therefore, CO₂, CH₄ and N₂ can be separated by a carbon membrane and silver-impregnated carbon membrane, which provide a new route for the separation. The larger the molecular kinetic diameter, the higher the permeance. Molecules of different sizes could be separated by this membranes because of differential time spent inside the membrane which excluded entrance of relatively larger molecules, allowing some entrance of medium-sized molecules, and free accessibility of the smallest molecules. The membrane contained the interconnected pores which the size can be controlled depending on the size of molecules to be separated. Smaller molecules (CO₂) experienced a more complex pathway (like a maze) to exit the particle than do larger molecules (N₂ and CH₄). Since fewer amount of large molecule could enter the pores, these larger size molecules elute first from

the column similar to the size exclusion chromatography technique. as shown in Figure 4.14a.

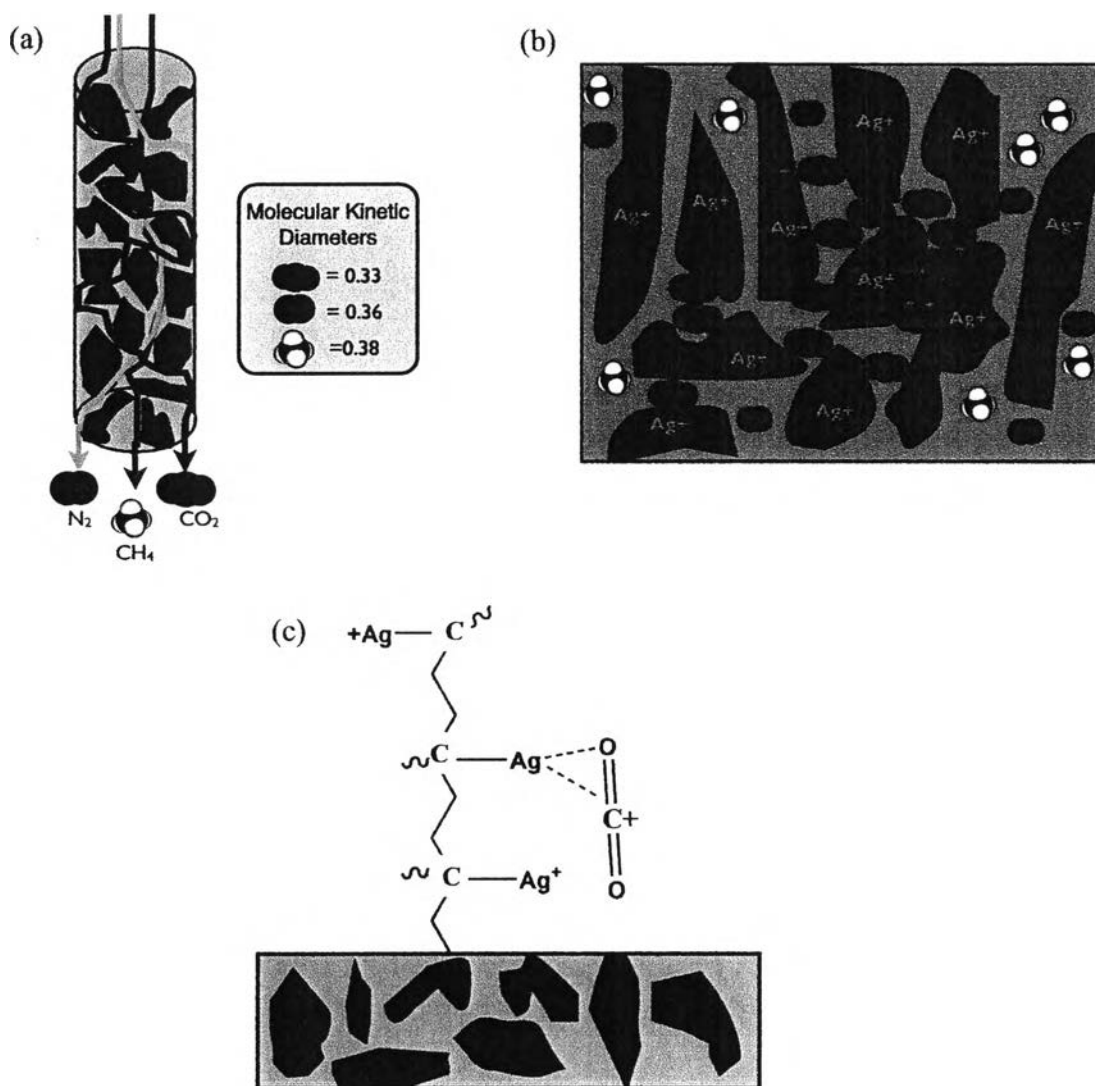


Figure 4.14 Pathway of gases depending on molecular kinetic diameter (a), complex formation between CO_2 and silver (b) and formation of π -bonded between CO_2 and double bond (c)

The CO₂ permeability in silver-impregnated carbon membrane decreased significantly with the AgNO₃ concentrations. CO₂ contained double bonds which could react reversibly with the silver ions and form the π -bonded complex, resulting in the low permeance as shown in Scheme 4.14b and 4.14c.

All these properties indicated that the gases sieved by the interconnected pores and the gas permeation was controlled by the molecular kinetic diameter of penetrant gas. Furthermore, the permeance was decreased by the silver inclusion.

4.4.6.2 The effect of silver inclusion on the selectivity

The CO₂/CH₄, CH₄/N₂ and N₂/CO₂ selectivity for carbon-silver membrane at different impregnated concentrations are shown in Figure 4.8.

Figure 4.15 shows the CO₂/CH₄ and N₂/CO₂ selectivity increased with an increase in the AgNO₃ concentrations. However, the silver inclusion did not enhance CH₄/N₂ selectivity. This is due to molecular sieving mechanism of porous structure compared to kinetic diameter of CO₂, N₂ and CH₄ molecules.

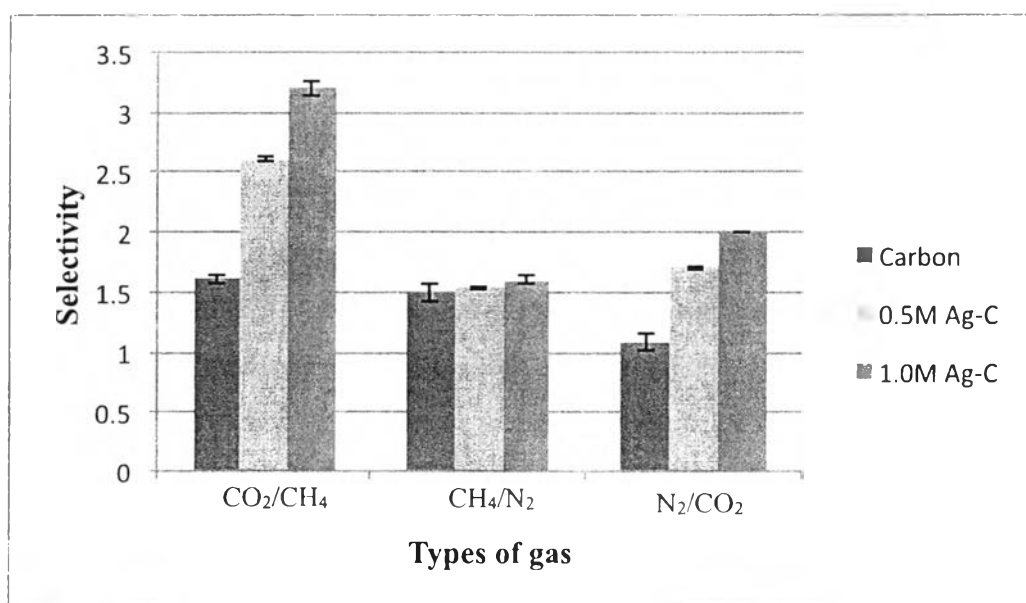


Figure 4.15 Effects of silver inclusion on CO₂/CH₄, CH₄/N₂ and N₂/CO₂ selectivity.

Conclusions

1.0CX-Ag, 0.5CX-Ag and CX were successfully synthesized via ambient drying by using polybenzoxazine as a precursor. The char yield of AgNO₃ impregnated polybenzoxazine xerogel was significantly increased with the increase of Ag content. The 1.0CX-Ag membrane showed the highest selectivity when compared with CX and 0.5CX-Ag membranes. Increasing the AgNO₃ concentrations significantly improve the gas permeability. The gas permeation was controlled by the molecular kinetic diameter of penetrant gas.

Acknowledgements

I am grateful for the scholarship and funding of the thesis work provided by the Petroleum and Petrochemical College, and by the Center of Excellence on Petrochemicals, and Materials Technology, Thailand.

References

- [1] Clarkson, C.R. and Bustin, R.M. (1999) Binary gas adsorption-desorption isotherms: effect of moisture and coal composition upon carbon dioxide selectivity over methane. *International Journal of Coal Geology*, 42, 241–271.
- [2] Gruskiewicz, M.S., Naney, M.T., Blencoe, J.G., Cole, D.R., Pashin, J.C. and Carroll, R.E. (2009) Adsorption kinetics of CO₂, CH₄, and their equimolar mixture on coal from the Black Warrior Basin, West-Central Alabama. *International Journal of Coal Geology*, 77, 23–33.
- [3] Şen, D., Kalıpçılar, H., and Yilmaz, L. (2007). Development of polycarbonate based zeolite 4A filled mixed matrix gas separation membranes. *Journal of Membrane Science*, 303, 194-203.
- [4] Hashemifard, S.A., Ismaila, A.F. and Matsuura, T. (2011). Mixed matrix membrane incorporated with large pore size halloysite nanotubes (HNTs) as filler for gas separation: Morphological diagram. *Chemical Engineering Journal*, 172, 581-590.
- [5] Chung, T.S., Jianga, L.Y., Lia, Y., and Kulprathipanj, S. (2007). Mixed matrix membranes (MMMs) comprising organic polymers with dispersed inorganic fillers for gas separation. *Progress in Polymer Science*, 32, 483–507.

- [6] Reijerkerk, S.R., Nijmeijer, K., Ribeiro Jr., C.P., Freeman B.D., and Wessling M. (2011) On the effects of plasticization in CO₂/light gas separation using polymeric solubility selective membranes. *Journal of Membrane Science*, 367, 33-44.
- [7] Ismail, A.F., and David, L.I.B. (2001) A review on the latest development of carbon membranes for gas separation. *Journal of Membrane Science*, 193, 1-18.
- [8] Kim, Y.Y., Park, H.B., Lee, and Y.M. (2004) Carbon molecular sieve membranes derived from thermally labile polymer containing blend polymers and their gas separation properties, *Journal of Membrane Science*. 243 (2004) 9–17.
- [9] Low B.T., Chung, T.S. (2011) Carbon molecular sieve membranes derived from pseudo- interpenetrating polymer networks for gas separation and carbon capture, *Carbon*, 49, 2104–2112.
- [10] He, X., Hagg, M.B. (2010) Hollow fiber carbon membranes: investigations for CO₂ capture, *Journal of Membrane Science*, doi:10.1016/j.memsci.2010.10.070.
- [11] Hosseini, S.S., and Chung, T.S. (2009) Carbon membranes from blends of PBI and polyimides for N₂/CH₄ and CO₂/CH₄ separation and hydrogen purification. *Journal of Membrane Science*, 328, 174-185.
- [12] Song, C.W., Wang, T.H., Qiu, Y.H., Qiu, J.S., and Cheng, H.M. (2009) Effect of carbonization atmosphere on the structure changes of PAN carbon membranes, *J. Porous Mater.* 16, 197–203.
- [13] A.J. Bird, D.L. Trimm, (1983) Carbon molecular sieves used in gas separation membranes, *Carbon*, 21, 177.
- [14] Centeno, T.A., Vilas, J.L., and Fuertes, A.B. (2004) Effects of phenolic resin pyrolysis conditions on carbon membrane performance for gas separation, *Journal of Membrane Science*, 228, 45–54.
- [15] Wei, W., Qin, G.T., Hu, H.Q., You, L.B., and Chen, G.H. (2007) Preparation of supported carbon molecular sieve membrane from novolac phenol-formaldehyde resin, *Journal of Membrane Science*, 303, 80–85.

- [16] Liu, Y.L., Yu, J.M., and Chou, C.I. (2004). Preparation and properties of novel benzoxazine and polybenzoxazine with maleimide groups. Journal of Polymer Science, 42, 5954-5963.
- [17] Li, Y., and Chung, T.S. (2007) Novel Ag⁺-zeolite/polymer mixed matrix membranes with a high CO₂/CH₄ selectivity. AIChE. Journal, 53(3), 610-616.
- [18] Takeichi, T., Kano, T., and Agag, T. (2005) Synthesis and thermal cure of high molecular weight polybenzoxazine precursors and the properties of the thermosets. Polymer, 46, 12172–12180.
- [19] Katanyoota, P., Chaisuwan, T., Wongchaisuwat, A., and Wongkasemjit, S. (2010) Novel polybenzoxazine-based carbon aerogel electrode for supercapacitors. Materials Science and Engineering B, 167, 36-42.
- [20] Low, H.Y., and Ishida, H. (1999) Structural effects of phenols on the thermal and thermo-oxidative degradation of polybenzoxazines. Polymer, 4365-4376.
- [21] Dunkers, J. and Ishida, H. (1995) Vibrational assignments of N,N-bis(3,5-dimethyl-2-hydroxybenzyl)methylamine in the fingerprint region. Spectrochimica Acta Part A: Molecular and Biomolecular Spectroscopy, 51, 1061-1074.
- [22] Low, H.Y., and Ishida H. (2006) Improved thermal stability of polybenzoxazines by transition metals. Polymer Degradation and Stability, 91, 805-815.
- [23] Lorjai, P., Chaisuwan, T., and Wongkasemjit, S. (2009). Porous structure of polybenzoxazine-based organic aerogel prepared by sol-gel process and their carbon aerogels. Journal of Sol-Gel Science and Technology, 52(1), 56-64.
- [24] Thubsuang, U., Ishida, H., Wongkasemjit, S., and Chaisuwan, T. (2012) Novel template confinement derived from polybenzoxazine-based carbon xerogels for synthesis of ZSM-5 nanoparticles via microwave irradiation. Microporous and Mesoporous Materials, 156, 7–15
- [25] Job, N., They, A., Pirard, R., Marien, J., Kocon, L., Rouzaud, J., Beguin, F., Pirard, J. (2005) Carbon aerogels, cryogels and xerogels: Influence of the drying method on the textural properties of porous carbon materials. Carbon, 43, 2481–2494.

- [26] Gregg, S.J., Sing, K.S.W. (1982) Adsorption, Surface Area and Porosity, 2nd ed., Academic Press, New York.
- [27] Rouquerol, F., Rouquerol, J., Sing, K.S.W. (1999) Adsorption by Powders and Porous Solids, Principles, Methodology and Applications, Academic press.